Hysteretic (Non-reversible) Bit-Rock Interaction Model for Torsional Vibration Analysis of a Drillstring

F. F. Real[1(✉)], A. Batou[2], T. G. Ritto[3], C. Desceliers[4], and R. R. Aguiar[5]

[1] National Institute of Metrology, Quality and Technology-INMETRO,
Rua Santa Alexandrina, 416, Rio de Janeiro, RJ 20261-232, Brazil
`ffreal@inmetro.gov.br`
[2] Department of Mechanical, Materials and Aerospace Engineering,
School of Engineering, University of Liverpool, Liverpool L69 7ZF, UK
`anas.batou@liverpool.ac.uk`
[3] Department of Mechanical Engineering, Federal University of Rio de Janeiro,
Ilha do Fundão, Rio de Janeiro, RJ 21945-970, Brazil
`tritto@mecanica.ufrj.br`
[4] Université Paris-Est, Laboratoire Modélisation et Simulation Multi Echelle,
MSME, UMR 8208 CNRS, 5 bd Descartes, 77454 Marne-la-Vallée, France
`christophe.desceliers@univ-paris-est.fr`
[5] Brazil Research and Geoengineering Center,
Schlumberger Oilfield Services, Rio de Janeiro, Brazil
`raguiar@slb.com`

Abstract. This paper aims at constructing a novel hysteretic (non-reversible) bit-rock interaction model for the torsional dynamics of a drillstring. Non-reversible means that the torque on bit is not represented only in terms of the bit speed, but also of the bit acceleration, producing a hysteretic behavior. Here, the drillstring is considered as a continuous system which is discretized by means of the finite element method, where a reduced-order model is applied using the normal modes of the associated conservative system. The nonlinear torsional vibrations of the drillstring system are analyzed comparing the proposed bit-rock interaction model to a commonly used reversible model (without hysteresis). The parameters of the proposed hysteretic bit-rock interaction and of the commonly used reversible model are fitted to field data. Results show the system including a bit-rock interaction model with hysteresis effects reproduces a good approach of stick-slip cycle, and the simulated drillstring dynamics using the bit-rock interaction presents a similar behavior comparing to the field data.

Keywords: Drill string nonlinear dynamics
Bit/rock interaction model · Torsional vibrations
Stick-slip oscillations · Stability map · Hysteresis

1   Introduction

Drillstring is a slender structure used for exploitation of oil reserves. It is composed mainly of two parts: drillpipes and bottomhole-assembly. A top drive rotates the system at the top, which transmits the torque to the bit that drills the rock. One of the concerns with the drillstring dynamics is its torsional vibrations that might lead to stick-slip oscillations [5, 8–10, 28]. In this severe conditions, the bit sticks (zero speed) then slips (high speed), and that might cause, for instance, measurement equipment failure, low rate of penetration, bit damage, and fatigue [31].

Spanos et al. [27] has published an overview of drilling vibrations. Specially for bit-rock interaction during the drilling process, [18, 24] have shown that the torque on bit varies nonlinearly with the bit speed, presenting large fluctuations. Concerning drillstring torsional dynamics and stick-slip oscillations, several papers discuss about them [8, 9, 15, 16, 23, 24, 29], and normally a pure torsional model is enough to represent this kind of system: to represent test rigs, [15] applied a torsional model successfully to analyze the friction-induced limit cycling, and in [9] a torsional model is used to implement a control strategy. Field data of a five kilometer drill string is analyzed in [24], where again a pure torsional model presented satisfactory results reproducing field data, where torsional vibration was the dominant phenomenon observed. More generally, a coupled axial-lateral-torsional model should be applied [23, 28].

There are many phenomena involved during the drilling process: fluid-rock interaction, proper well profile (inclination and azimuth), pipe-rock interaction, among others. Therefore, a full description model of bit-rock interaction including all dynamics is really hard to obtain due to lack of downhole data. Experimentally, hysteretic cycles for the bit-rock interaction were observed in [11, 18–20], which can be caused by tangential stiffness during the bit-rock interaction, and by the frictional memory due a delay in the friction force, being evident during the stick phase and the switch between stick and slip phases [30]. Although of these observations, up to the authors knowledge the only hysteretic bit-rock interaction model found in the literature was proposed in [5]. The authors in [5] used the experimental results presented in [11], and applied their hysteretic model, which employs a switching mechanism, in the analysis of Proportional-Integral (PI) control strategy, aiming at mitigating stick-slip oscillations.

This paper aims at constructing a novel hysteretic (non-reversible) bit-rock interaction model for the torsional dynamics of a drillstring [19] based on the field data presented in [24]. Non-reversible means that the torque on bit is not represented only in terms of the bit speed, but also of the bit acceleration, producing a hysteretic behavior. The drillstring is considered as a continuous system which is discretized by means of the finite element method [6, 7, 25], where a reduced-order model is applied using the normal modes of the associated conservative system. The nonlinear torsional vibrations of the drillstring system are analyzed comparing the proposed bit-rock interaction model to a commonly used reversible model (without hysteresis). Least-Square method is used for parame-

ter identification is applied to obtain the parameters of the models according to field data [24].

The main contribution of this paper is to propose an original model for the bit-rock interaction taking into account the hysteretic effects. Here, (1) a new nonlinear hysteretic model is constructed to describe the bit-rock interaction (nonlinear torque function) as a function of the bit speed and bit acceleration, (2) experimental identification using Least-Square method is applied to obtain the parameters of the mean nonlinear part, and (3) a hysteretic function is proposed for the envelope of this process, which is also a function of the acceleration and bit speed.

This article is organized as follows. The drillstring torsional dynamical model is presented in Sect. 2.1. The continuous system is discretized by means of the finite element method and a reduced-order model is constructed using the normal modes of the associated conservative system. In Sect. 2.1, the proposed bit-rock interaction model including hysteresis is also presented, as well as the reversible model (without hysteresis). This proposed model is compared with field data in Sect. 5. The numerical analysis are presented in Sect. 6 and, finally, the concluding remarks are made in Sect. 8.

2   Dynamical Model

2.1   Torsional Model

As mentioned before, the drillstring is basically composed by (1) the drillpipes (DP) and (2) the bottomhole-assembly (BHA), as it is schematically represented in Fig. 1. DP are slender tubes that can reach kilometers, while BHA is composed by thicker tubes (drill collars) together with the measurement equipment and a drill bit on its bottom, and its length can reach hundreds of meters.

A vertical wellbore is considered, and only torsional vibrations are taken into account in the modeling. That is, it is assumed that there are no contact between the column and the wellbore, as well as the lateral and axial vibrations are small. A constant speed Ω is imposed at the top and a reaction torque appears due to the bit-rock interaction. Therefore, $\boldsymbol{\theta}(x,t)$ is the solution of the following boundary value problem:

$$\rho I_p \frac{\partial^2 \boldsymbol{\theta}(x,t)}{\partial t^2} - G I_p \frac{\partial^2 \boldsymbol{\theta}(x,t)}{\partial x^2} = \boldsymbol{T}(x,t), \tag{1}$$

in which the boundary conditions are

$$\begin{cases} \boldsymbol{\theta}(0,t) = \Omega t \\ \dot{\boldsymbol{\theta}}(0,t) = \Omega \end{cases}, \tag{2}$$

and the initial conditions are

$$\boldsymbol{\theta}(x,0) = 0, \quad \dot{\boldsymbol{\theta}}(x,0) = \Omega, \tag{3}$$
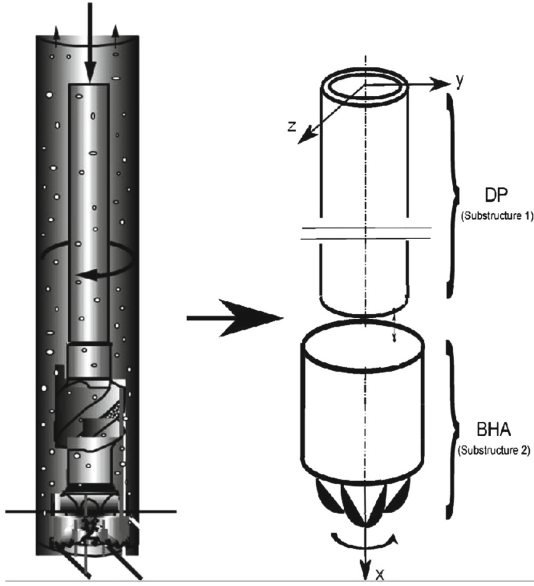
Fig. 1. General scheme of a drillstring.

where $\boldsymbol{\theta}(x,t)$ is the angular rotation about the x-axis, $\boldsymbol{T}(x,t)$ is the torque vector, I_p is the cross sectional polar moment of inertia, and ρ and G are the density and shear modulus of the material of the column.

Different from [21, 22], the present paper will solve the system considering its rotational displacements about a rotating frame. Let $\boldsymbol{\theta}^{rel}(x,t)$ be the relative torsional degree of freedom in the rotating frame associated to the top sectional area (at x = 0). We introduce the absolute rotational displacement as

$$\boldsymbol{\theta}(x,t) = \Omega t + \boldsymbol{\theta}^{rel}(x,t). \tag{4}$$

Let $\boldsymbol{u}(t)$ be the vector of $\boldsymbol{\theta}^{rel}(x,t)$ nodal values of a mesh of the drillstring. A computational model is constructed by the finite element method considering the drillstring top clamped (there is not relative displacement between the top drive and the first element on the top of the drillstring). Adding a proportional damping to the system, the vector $\boldsymbol{u}(t)$ is solution of the non-linear differential equation

$$[M]\ddot{\boldsymbol{u}}(t) + [D]\dot{\boldsymbol{u}}(t) + [K]\boldsymbol{u}(t) = \boldsymbol{T}(\dot{\boldsymbol{u}}(t)), \tag{5}$$

with the initial conditions

$$\boldsymbol{u}(0) = \boldsymbol{0}, \quad \dot{\boldsymbol{u}}(0) = \boldsymbol{0}. \tag{6}$$

where $[M]$ is the mass matrix, $[D]$ is the damping matrix, $[K]$ is the stiffness matrix, and $\boldsymbol{T}(\dot{\boldsymbol{u}}(t))$ is the generalized torque vector. All the components of generalized torque vector are zero except the one corresponding to the drill bit.

The nonlinear torque applied to the bit (corresponding to the drillstring's length equal to L) is denoted by $\bar{T}_{bit}(\dot{\boldsymbol{\theta}}_{bit}(t))$ and will be described further in this text.

The normal modes of the conservative homogeneous system are used to construct a reduced-order model. The m first eigenvalues $0 < \lambda_1 \leq \lambda_2 \leq \ldots \leq \lambda_m$ associated with elastic modes $\{\boldsymbol{\phi}_1, \boldsymbol{\varphi}_2, \ldots, \boldsymbol{\varphi}_m\}$ are solutions of the generalized eigenvalue problem

$$[K]\,\boldsymbol{\varphi} = \lambda[M]\,\boldsymbol{\varphi}. \tag{7}$$

The reduced-order model is obtained by projecting the full computational model on the subspace spanned by the m first elastic modes calculated using Eq. (7). Let $[\Phi]$ be $n \times m$ matrix whose columns are the m first elastic modes. We can then introduce the following approximation

$$\boldsymbol{u}(t) = [\Phi]\,\boldsymbol{q}, \tag{8}$$

in which $\boldsymbol{q}$ is the vector of the m generalized coordinates which are solution of the reduced matrix equation

$$[\widetilde{M}]\ddot{\boldsymbol{q}}(t) + [\widetilde{D}]\dot{\boldsymbol{q}}(t) + [\widetilde{K}]\boldsymbol{q}(t) = \tilde{\boldsymbol{T}}(\dot{\boldsymbol{q}}(t)), \tag{9}$$

with the initial conditions

$$\boldsymbol{q}(0) = \boldsymbol{0}, \quad \dot{\boldsymbol{q}}(0) = 0. \tag{10}$$

In these equations, $[\widetilde{M}] = [\Phi]^T\,[M]\,[\Phi]$, $[\widetilde{D}] = [\Phi]^T\,[D]\,[\Phi]$ and $[\widetilde{K}] = [\Phi]^T\,[K]\,[\Phi]$ are $m \times m$ mass, damping and stiffness reduced-order matrices, and where $\tilde{\boldsymbol{T}}(\dot{\boldsymbol{q}}(t)) = [\Phi]^T\boldsymbol{f}([\Phi]\dot{\boldsymbol{q}}(t))$ is the vector of the reduced-order generalized torque. The set of Eqs. (8), (9) and (10) can be solved using commonly used integration schemes, such as the Euler scheme or the Runge-Kutta, for instance.

3   Deterministic Model - A Reversible Model

Now, let us introduce the deterministic bit-rock interaction model. This model introduced by Eq. 11 represents an average approximation of stick-slip behavior, that means a reversible model. The following nominal bit-rock interaction model is presented in [8,25,28] which combines Coulomb friction (hyperbolic tangent behavior), Stribeck friction (negatively sloped behavior), and viscous friction (directly proportional to the bit speed):

$$\bar{T}_{bit}(\dot{\theta}_{bit}(t)) = \alpha_0 \left[(\tanh(\alpha_1\,\dot{\theta}_{bit}(t)) + \frac{\alpha_2\,\dot{\theta}_{bit}(t)}{1 + \alpha_3\,\dot{\theta}_{bit}^2(t)} \right], \tag{11}$$

where α_0, α_1, α_2, and α_3, are calibration parameters of this model with appropriate units. All these parameters must be identified experimentally, and α_0 is a remarkable parameter because of its dependence of weight on bit and friction coefficient.

4   Hysteretic Model

Stick-slip is a self-excited drilling torsional oscillation due the friction between the bit and the rock, because of the cumulative of energy throughout the drill-string (top drive does not stop during the stick phase). This energy induces the slip phase behavior, which is released promoting the acceleration of bit above the top drive acceleration. This oscillation reaches a maximum value of the bit speed during this cycle, decelerating after that.

Therefore, these stick-slip oscillations can present a hysteretic behavior, which is formed by two motion phenomenons: one of microscopic magnitude (being evident during the stick phase), and another one of macroscopic magnitude (being evident during the switch between stick and slip phases). This microscopic motion phenomenon is caused by tangential stiffness during the interaction between the bodies [1,3,12–14]. The macroscopic motion phenomenon is related to the frictional memory due a delay in the friction force, where the size of the loops increase according to the angular velocity variations become faster [4,17], that means according to the acceleration.

Let $\dot{\theta}_{bit}(t)$ be the absolute angular speed at the bit. As a first attempt, we propose the following model for bit-rock interaction considering hysteretic effects:

$$T_{bit}(\dot{\theta}_{bit}(t),t) = \left[\bar{T}_{bit}(\dot{\theta}_{bit}(t))\right](H\eta(\dot{\theta}_{bit}(t)),\ddot{\theta}_{bit}(t)))), \tag{12}$$

in which

(1) $\bar{T}_{bit}(\dot{\theta}_{bit}(t))$ is the deterministic bit-rock interaction model considering hysteretic effects;
(2) $H\eta(\dot{\theta}_{bit}(t)),\ddot{\theta}_{bit}(t)))$ is the hysteresis function;
(3) $\ddot{\theta}_{bit}(t))$ is the instantaneous bit acceleration in hysteresis function. The hysteretic effect can be described by a simple function $(H\eta(\dot{\theta}_{bit}(t)),\ddot{\theta}_{bit}(t))))$ that depends on the instantaneous bit acceleration $\ddot{\theta}_{bit}(t)$ (see 13), as follows [19],

$$H\eta(\dot{\theta}_{bit}(t)),\ddot{\theta}_{bit}(t))) = 1 + sign(\dot{\theta}_{bit}(t))\gamma_1\tanh(\gamma_2\ddot{\theta}_{bit}(t)) \tag{13}$$

where γ_1 and γ_2 are calibration parameters related to the hysteresis effects with appropriate units.

This simple function is dependent of the instantaneous bit acceleration $\ddot{\theta}_{bit}(t))$, which can be obtained by the differential of $\dot{\theta}_{bit}(t)$ related to time. It is noticed that the hysteresis function has a hyperbolic tangent term instead of $sign\ddot{\theta}_{bit}(t))$, because of function's smoothness, and due its simplicity can be applied in another deterministic models of bit-rock interaction [19].

5   Bit-Rock Interaction: Proposed Model vs. Field Data

Field data (downhole information) presented in [24] are considered in this paper, which were acquired using a downhole mechanics measurement unit capable of
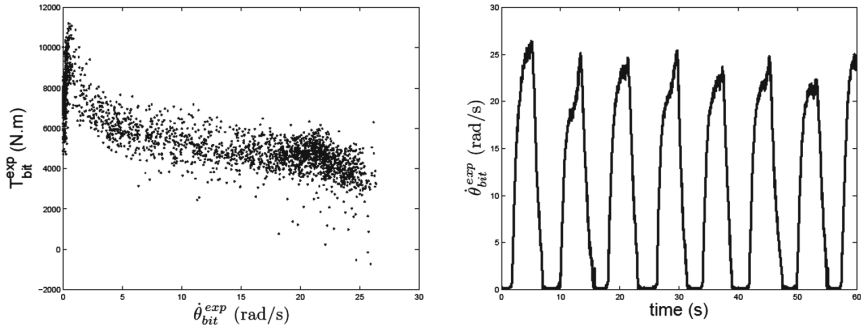
Fig. 2. Experimental torque on bit versus bit speed filtered prior to recording at 50 Hz, and bit speed related to time of sampling, both were reproduced from [24] graphs.
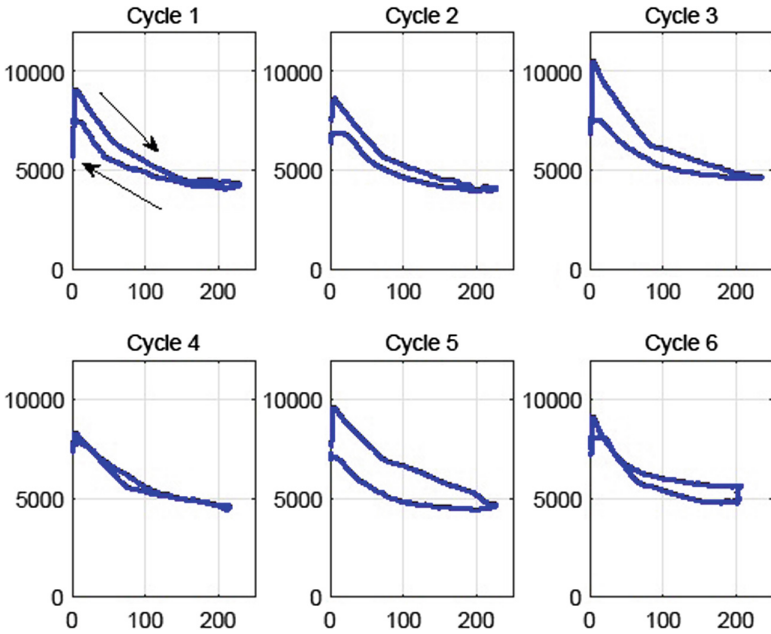

Fig. 3. Experimental torque on bit, bit speed, torque on bit versus bit speed and bit acceleration in 6 stick-slip cycles over a regular grid (395 records), and its sliding-window average,using a length equal to 0.01 rad/s (395 records).

providing both real-time measurement through mud telemetry and continuously recorded high-frequency data throughout the run. This unit was installed at the BHA above the bit with a suite of 19 sensors, which are able to sample triaxial accelerations, gyro rpm, magnetometer rpm, axial loading, torque, bending moment [26] at 10,000 Hz. These data are filtered prior to recording at 50 Hz.

Figure 2 shows the field data measurements reproduced from [24], where the imposed angular rotation at the top is $\Omega = 12.57\,\mathrm{rad/s}$ (120 RPM). Figure 2 shows how the torque increases when the bit sticks, and the bit speed alternates stick phases (almost zero speed) and slip phases (high speeds).

Field data showed here correspond to one sample, and statistic characteristics depend on the number of samples for being representative. To circumvent this limitation, let us avail each stick-slip cycle. If we consider that each slip phase depends exclusively on the previous stick phase, all the stick-slip cycles are independents. In that case, each stick-slip cycle can be considered one sample, being possible to construct statistic characteristics. Figure 3 separates the stick-slip cycles over a regular grid of 395 records in each stick-slip cycle within the range $[0, 7.9]\,\mathrm{s}$, despising the first and the last stick-slip cycle showed in Fig. 2.

Field data presented in this section show large fluctuations of the torque on bit. To have a closer look at these fluctuations and the hysteresis behavior, Fig. 3 shows the experimental measurements for one stick-slip cycle $(T_{bit}^{exp}(t))$ for each cycle, and for bit acceleration. Despite of the independence of stick-slip cycles, it can be seen that the torque fluctuations are not uncorrelated, i.e., it confirms that there is a correlation structure of the random process. The averages $T_{bit}^{SWAexp}(t)$ and $\ddot{\theta}_{bit}^{SWAexp}(t)$ are obtained by sliding-window method (SWA) [2], using a length equal to $0.01\,\mathrm{rad/s}$.

6   Numerical Results

Figure 4 shows the revisited experimental records (only 6 stick-slip cycles) of the bit-rock interaction with respect to the bit speed $(T_{bit}^{exp,rev})$, together with its revisited sliding-window average over the time domain [2], and the hysteretic fitted model $(T_{bit}^{Exp\,data\,applied\,to\,Identified\,model})$. These parameters are fitted using the least square method. This interaction model is supported by measurements [18,24]. The identified parameters for hysteresis function are given by $\gamma_1 = 1.95$, and $\gamma_2 = 3.00 \times 10^{-3}$, which are the average from identified values of the torque on bit fluctuations in each cycle. The identified values for $\alpha_{i,i=0,\dots,3}$ calibration parameters are $\alpha_0 = 4,705.80$, $\alpha_1 = 8,105.70$, $\alpha_2 = 4.02$, and $\alpha_3 = 4.00$. The averages (blue lines) are obtained by sliding-window method using a width equal to $0.01\,\mathrm{rad/s}$.

Figure 5 shows the hysteretic behavior from the model over a regular grid, in order to check the mirrored offset of the curve, respecting the three models of friction considered in this work (Coulomb friction, Stribeck friction, and viscous friction models).

Figure 6 shows a reasonable agreement between the model and average experimental bit-rock interaction. Nevertheless, it can be seen that the experimental data show large fluctuations and a stochastic model for the bit-rock interaction could be used to improve the model predictions of the drillstring dynamics.
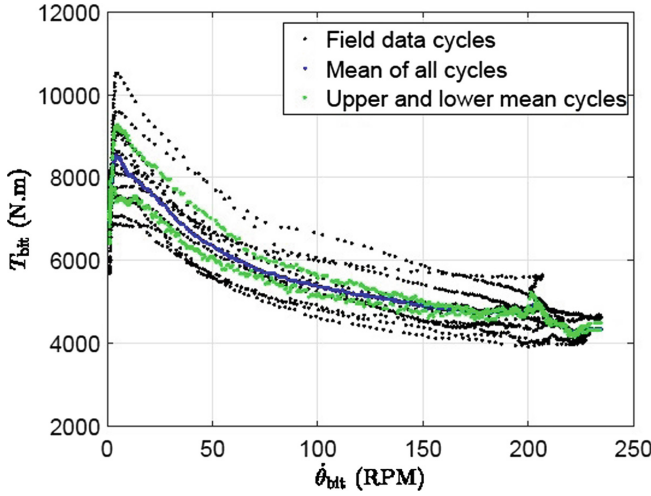
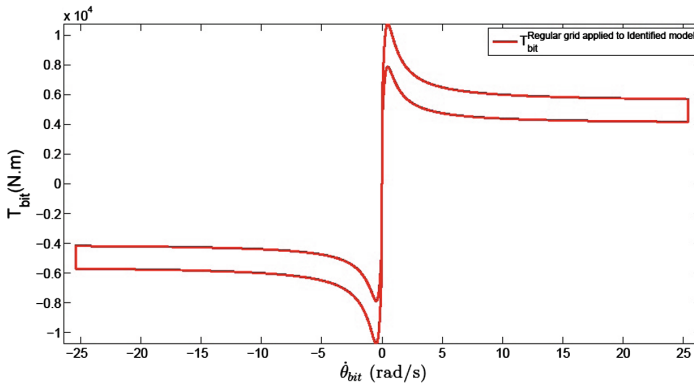**Fig. 4.** Experimental bit-rock interaction and identified average model.

Fig. 5. Hysteretic behaviour of the bit-rock interaction from the model over a regular grid.

7   Simulation of the Torsional Dynamics

The drillstring dynamics is simulated in the condition of the experimental data. Table 1 contains the parameters of the drillstring used for the simulation.

The mass and stiffness matrices are constructed using 100 finite elements (linear shape functions). The generalized damping matrix is diagonal with damping ratios equal to 0.005 for the first mode, 0.03 for the second and third modes, and 0.005 for all the other modes. The non-linear Eq. (9) is solved using a modified Euler scheme with a time step 0.512 ms.

As it is a first attempt to construct a stochastic model for the bit-rock interaction fitting field data, one realization of the computational model is compared
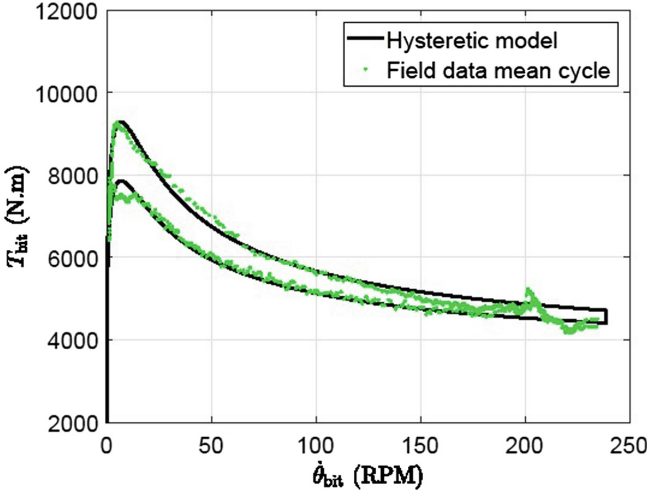
Fig. 6. Comparison between field data mean cycle and hysteretic model over a regular grid.

Table 1. Drillstring characteristics.

	DP	BHA
Elastic modulus [GPa]	220	220
Poisson's coefficient	0.29	0.29
Volumetric mass density [kg/m^3]	7,800	7,800
Length [m]	4,733.60	466.45
Inner radius [m]	0.0595	0.0363
Outer radius [m]	0.070	0.0803

with the experimental results. The idea is to verify if the numerical results can approximate the dynamic behavior observed in the field data.

Figure 7 compares the bit speed obtained by the computational model to with the field data. It is observed that the dynamic behavior is similar. Both dynamics present stick-slip oscillations and have a similar aspect, although the amplitude of the response of the computational model is a little higher than the field data for some cycles (almost 20% higher).

Finally, Fig. 8 shows a very good agreement between the bit-rock interaction model proposed herein and the field data. The simulated levels of fluctuation are in good agreement with experiments, albeit the numerical results shows torque values for higher bit speeds. And the cycle's trajectory has presented the same correlation tendencies as the experimental ones. The nominal bit-rock interaction model considered is a regularized Coulomb friction model with decreasing torque approaching the dynamic friction torque as the bit speed increases. Therefore,
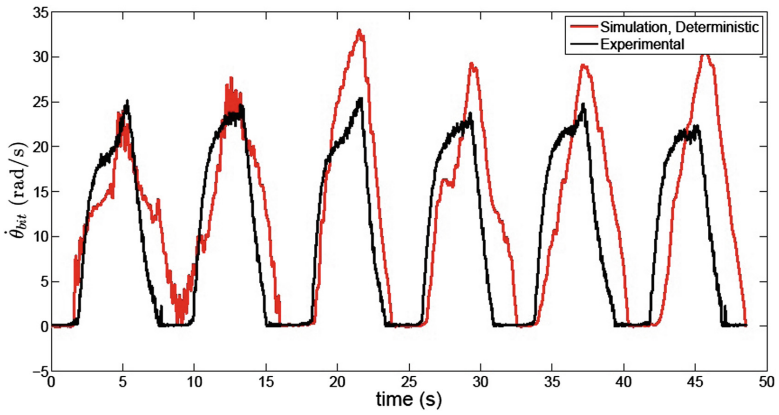
Fig. 7. Comparison between simulated and field data bit speed, where field data were reproduced from [24].
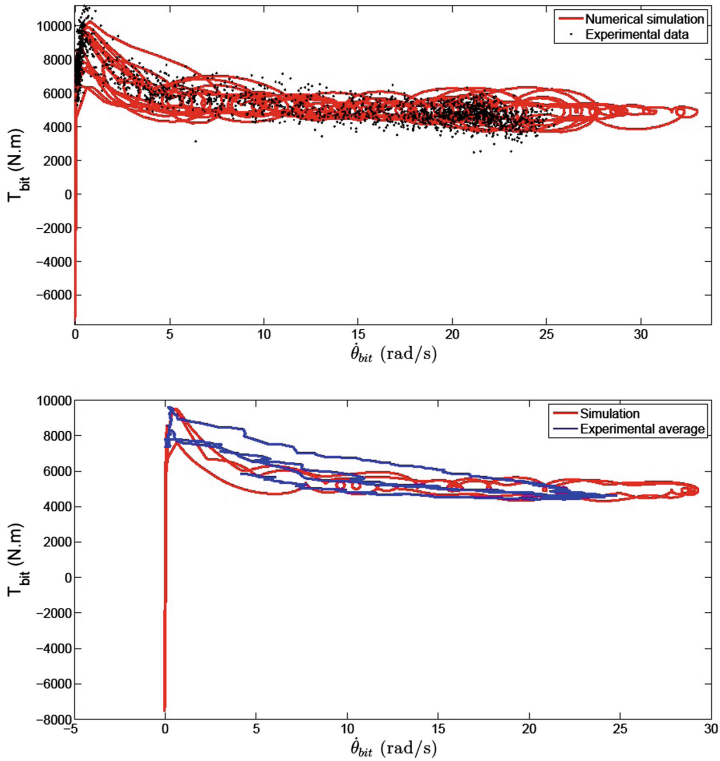

Fig. 8. Simulated bit-rock interaction and just one cycle within the range [20, 30] s.

the torque goes to zero when the bit speed approaches zero. Physically, when the bit sticks, the torque might assume any value from zero to its static friction limit. Hence, the difference in the results might be due to the deterministic model chose for the torque on bit.

8   Concluding Remarks

In this paper, a new modeling for the bit-rock interaction has been proposed considering hysteresis effects of friction. The proposed model depends on 6 parameters that can be fitted or used for a sensitivity analysis.

The torsional dynamics of the system is analyzed, which is represented as a torsion bar discretized by means of the finite element method. A reduced-order model was constructed to speed up the computations. On the bottom of this system, the proposed bit-rock interaction model with hysteresis effects is applied and this system is able to reproduce a good approach of stick-slip cycle.

The simulated drillstring dynamics using the bit-rock interaction presented a similar behavior comparing to the field data. Specially, the torque on bit as a function of the bit speed presented the same behaviour as the ones observed experimentally.

Future works concern the validation of the model through a series of laboratory experiments. It would be particularly interesting to investigate the influence of the (1) top speed Ω, (2) weight on bit, and (3) the rock characteristics. It would also be interesting to take into account uncertainties in the drillstring computational model and stochastic modeling of bit-rock interaction using hysteresis function.

References

1. Courtney-Pratt, J.S., Eisner, E.: The effect of a tangential force on the contact of metallic bodies. Philos. Trans. R. Soc. A: Math. Phys. Eng. Sci. **238**(1215), 529–550 (1956)
2. Chou, Y.: Statistical Analysis. Holt International, Canada (1975)
3. Harnoy, A., Friedlanf, B., Rachoor, H.: Modeling and simulation of elastic and friction forces in lubricated bearings for precise motion control. Wear **172**(2), 155–165 (1994)
4. Hess, D.P., Soom, A.: Friction at lubricated line contact operating at oscillating sliding velocities. J. Tribol. **112**, 147–152 (1990)
5. Hong, L., Girsang, I.P., Dhupia, J.S.: Identification and control of stick-slip vibrations using Kalman estimator in oil-well drillstrings. J. Pet. Sci. Eng. **140**, 119–127 (2016)

6. Jansen, J.D.: Nonlinear dynamics of oil well drill strings. Ph.D. thesis, Technische Universiteit Delft (1993)
7. Khulief, Y.A., Al-Naser, H.: Finite element dynamic analysis of drillstrings. Finite Elem. Anal. Des. **41**, 1270–1288 (2005)
8. Khulief, Y.A., Al-Sulaiman, F.A., Bashmal, S.: Vibration analysis of drillstrings with self-excited stick-slip oscillations. J. Sound Vib. **299**(3), 540–558 (2007)
9. Kreuzer, E., Steidl, M.: Controlling torsional vibrations of drill strings via decomposition of traveling waves. Arch. Appl. Mech. **82**(4), 515–531 (2012)
10. Leine, R.I., van Campen, D.H., van den Steen, L.: Stick-slip vibrations induced by alternate friction models. Nonlinear Dyn. **16**, 41–54 (1998)
11. Leine, R.I., van Campen, D.H., Keultjes, W.J.G.: Stick-slip whirl interaction in drillstring dynamics. J. Vib. Acoust. **124**, 209–220 (2002)
12. Liang, J.-W., Feeny, B.F.: Dynamical friction behaviour in a forced oscillator with compliant contact. J. Appl. Mech. **65**(1), 250–257 (1998)
13. Liang, J.-W., Feeny, B.F.: Identifying Coulomb and viscous friction from free-vibration decrements. J. Sound Vib. **282**(35), 1208–1220 (2005)
14. Liang, J.-W., Feeny, B.F.: A comparison between direct and indirect friction measurements in a forced oscillator. J. Appl. Mech. **65**(3), 783–786 (1998)
15. Mihajlovic, N., van De Wouw, N., Hendriks, M.P.M., Nijmeijer, H.: Friction-induced limit cycling in flexible rotor systems: an experimental drill-string set-up. Nonlinear Dyn. **46**(3), 273–291 (2006)
16. Navarro-López, E.M., Licéaga-Castro, E.: Non-desired transitions and sliding-mode control of a multi-DOF mechanical system with stick-slip oscillations. Chaos Solitons Fractals **41**(4), 2035–2044 (2009)
17. Olsson, H., Åström, K.J., Canudas de Wit, C., Gäfvert, M., Lischinsky, P.: Friction models and friction compensation. Eur. J. Control **4**(3), 176–195 (1998)
18. Pavone, D.R., Desplans, J.P.: Application of high sampling rate downhole measurements for analysis and cure of stick-slip in drilling. In: Proceedings - SPE Annual Technical Conference and Exhibition Delta, pp. 335-345 (1994)
19. Real, F.F., Batou, A., Ritto, T.G., Desceliers, C., Aguiar, R.R.: Hysteretic bit/rock interaction model to analyze the torsional dynamics of a drill string. Mech. Syst. Signal Process. **111**, 222–233 (2018)
20. Richard, T., Germay, C., Detournay, E.: A simplified model to explore the root cause of stick-slip vibrations in drilling systems with drag bits. J. Sound Vib. **305**(3), 432–456 (2007)
21. Ritto, T.G., Soize, C., Sampaio, R.: Non-linear dynamics of a drill-string with uncertain model of the bit-rock interaction. Int. J. Non-Linear Mech. **44**(8), 865–876 (2009)
22. Ritto, T.G., Sampaio, R.: Stochastic drill-string with uncertainty on the imposed speed and on the bit-rock parameters. Int. J. Uncertain. Quantif. **2**(2), 111–124 (2012)
23. Ritto, T.G.: Bayesian approach to identify the bit-rock interaction parameters of a drill-string dynamical model. J. Braz. Soc. Mech. Sci. Eng. **37**(4), 1173–1182 (2015)
24. Ritto, T.G., Aguiar, R.R., Hbaieb, S.: Validation of a drill string dynamical model and torsional stability. Meccanica **52**, 2959–2967 (2017)
25. Sampaio, R., Piovan, M.T., Lozano, G.V.: Coupled axial/torsional vibrations of drilling-strings by mean of nonlinear model. Mech. Res. Comun. **34**(5–6), 497–502 (2007)

26. Shi, J., Durairajan, B., Harmer, R., Chen, W., Verano, F., Arevalo, Y., Douglas, C., Turner, T., Trahan, D., Touchet, J., Shen, Y., Zaheer, A., Pereda, F., Robichaux, K., Cisneros, D.: Integrated efforts to understand and solve challenges in 26-in salt drilling, Gulf of Mexico. In: SPE 180349-MS, SPE Deepwater Drilling and Completions Conference, Galveston, Texas, USA (2016)
27. Spanos, P.D., Chevalier, A.M., Politis, N.P., Payne, M.L.: Oil and gas well drilling: a vibrations perspective. Shock Vib. Dig. **35**(2), 85–103 (2003)
28. Tucker, R.W., Wang, C.: An integrated model for drill-string dynamics. J. Sound Vib. **224**(1), 123–165 (1999)
29. Viguié, R., Kerschen, G., Golinval, J.-C., McFarland, D.M., Bergman, L.A., Vakakis, A.F., van de Wouw, N.: Using passive nonlinear targeted energy transfer to stabilize drill-string systems. Mech. Syst. Signal Process. **23**(1), 148–169 (2009)
30. Wojewoda, J., Stefaski, A., Wiercigroch, M., Kapitaniak, T.: Hysteretic effects of dry friction: modelling and experimental studies. Philos. Trans. R. Soc. A: Math. Phys. Eng. Sci. **366**(1866), 747–765 (2008)
31. Wu, X., Karuppiah, V., Nagaraj, M., Partin, U.T., Machado, M., Franco, M., Duvvuru, H.K.: Identifying the root cause of drilling vibration and stick-slip enables fit-for-purpose. In: IADC/SPE Drilling Conference and Exhibition, no. 151347 (2012)